International Journal of Dynamics and Control (2019) 7:295–307
https://doi.org/10.1007/s40435-018-0447-6

Robust output feedback control of electro-hydraulic system

Ashpana Shiralkar[1] · Shailaja Kurode[2] · Ruchira Gore[3] · Bhagyashri Tamhane[2]

Received: 16 December 2017 / Revised: 31 May 2018 / Accepted: 6 June 2018 / Published online: 13 June 2018

Abstract

This paper presents output feedback second order sliding mode control to achieve robust finite time position control for Electro-Hydraulic Servo System (EHSS). The system is subjected to inherent uncertainties, parametric perturbations and disturbances. A nonlinear dynamics of EHSS is represented by linear uncertain dynamics for the sake of control design. A relative degree one sliding surface is proposed. It is shown that super twisting controller using this relative degree one sliding surface attains finite time positioning. Further disturbance estimation is used to augment the control for getting desired performance with less control effort. The method is validated in simulation and experiment both. The performance of the proposed controller is compared with the super twisting controller devised using non singular terminal sliding surface which also yields finite time positioning.

Keywords Electro-Hydraulic Servo System (EHSS) · Second Order Sliding Mode Control (SOSMC) · Finite time control

List of symbols

v	Applied voltage (V)
i	Current through coil (A)
R	Resistance of coil (Ω)
$L(x_s)$	Inductance of coil which is a function of spool displacement x_s (H)
N	Number of turns in coil
R_l	Total reluctance (Mho)
μ_0	Magnetic permeability (N/A^2)
μ_r	Relative permeability of ferromagnetic material (N/A^2)
A_p	Cross section area of plunger (m^2)
l_p	Length of plunger (m)
l_a	Air gap length (m)
x_s	Spool-plunger displacement (m)
m_s	Mass of (plunger + spool) assembly (kg)
b	Damping coefficient of spool (Ns/m)
k	Spring coefficient of spool (N/m)
q_1, q_2	Flow rate in chamber 1 and 2 (m^3/s)
c_d	Flow discharge coefficient
ω	Area gradient (m^2/m)
p_s	Supply pressure of system (N/m^2)
p_1, p_2	Pressure in chamber 1 and chamber 2 (N/m^2)
v_1, v_2	Volume in chamber 1 and 2 (m^3)
v_i, v_f	Initial volume in chamber 1 and final volume in chamber 2 (m^3)
A_a	Cross sectional area of piston in chamber 1 (m^2)
A_b	Cross sectional area of piston in chamber 2 (m^2)
v_{p_1}, v_{p_2}	Volume of chamber 1 and 2 of pressure port (m^3)
ρ	Density of hydraulic fluid used (kg/m^3)
β	Bulk modulus of hydraulic fluid (N/m^2)
x_l	Load displacement (m)
m_l	Mass of load (kg)
b_l	Damping coefficient of load (Ns/m)

The authors would like to acknowledge the financial support of the Board of College and University Development, Savitribai Phule Pune University (SPPU), Pune through its research Project Ref No. OSD/BCUD/113/10.

✉ Ashpana Shiralkar
shiralkarashpana@gmail.com

Shailaja Kurode
srk.elec@coep.ac.in

Ruchira Gore
ruchiragore7@gmail.com

Bhagyashri Tamhane
t_bhagyashri@yahoo.co.in

[1] Department of Electrical Engineering, College of Engineering, Pune and Faculty at EED, AISSMS's IOIT, Pune, India

[2] Department of Electrical Engineering, College of Engineering, Pune, India

[3] Honeywell Automation Pvt. Ltd., Pune, India

1 Introduction

Electro-Hydraulic Servo System (EHSS) is well known for high torque to weight ratio and faster response. These features resulted in its use in many applications such as manufacturing systems, suspension systems, mining machinery, robotics, automotive industries and many more. In EHSS electrical signal plays an important role to accomplish flexible and accurate hydraulic actuation. Various methods of modeling have been examined by many researchers see for example [1–4] and the references therein.

Various control strategies have been reported in the literature for position control of EHSS. Proportional Integral Derivative (PID) controller is the classical controller and is widely used [5]. It has advantages such as simplicity, good stability, high reliability etc. However, tuning of PID gains and robustness of controller are the issues. Therefore, the conventional PID controller often cannot ensure the desired performance. Many methods have been proposed for improving PID controller. Still disturbance rejection and plant uncertainties tolerance beg a question.

For position control of EHSS neural network [6], fuzzy logic [7], feedforward [8] and Lyapunov [9] based control algorithms have been designed and implemented. Advanced control methods such as QFT [10], H_∞ [11] have been examined for EHSS. However, controller order becomes large and tuning of controller parameter becomes cumbersome. Adaptive control yields robust performance but needs exact knowledge of uncertainties and nonlinearities. Some authors combined adaptive control schemes with other techniques which include feedback linearization [12], backstepping [13], model reference adaptive control (MRAC) [14]. However, these control methods require linear parameterizations of the unknown parameters and exact knowledge of the nonlinear functions. Sliding mode control (SMC) is one of the robust control techniques reported in [15–19]. Although SMC gives robust performance against matched uncertainties and disturbances, chattering is the issue which is addressed using Higher Order Sliding Modes (HOSM) [20,21]. For the EHS system, the proposed HOSM control is complimented with disturbance observer (DO) for an efficient control design. DO is mathematically an inversion of system dynamics and is one of the simplest disturbance estimator designed to estimate disturbance and accommodating control strategy proposed by Johnson [22]. The origin of DO can be traced to [23] by Ohishi, in which estimation using disturbance decoupling has been proposed. A similar basic DO is proposed for EHS system, in this paper.

1.1 Motivation

Research on the modeling and control of electro-hydraulic systems has received sustained attention due to their several advantages. Need to provide desired performance in the presence of nonlinearities in the valve, spool, pressure dynamics of EHSS has been motivation for investigation of a robust control method. Often model approximation is used to simplify control design. However, it leads to performance degradation. It is required to design a control which takes care of wide varieties of uncertainties. SMC is robust. However, it suffers a drawback of chattering. Higher Order Sliding Mode Control (HOSMC) has evolved to yield robust performance and smooth control. This has been motivated us to examine HOSM controller.

The Super-Twisting Algorithm (STA) is one of the best Second Order Sliding Mode Control (SOSMC) algorithms [24]. Some of the researchers have examined SOSMC for EHSS [25,26]. However, while developing mathematical modeling the authors have not considered the solenoid coil nonlinearities which has been considered in the present work. The preliminary version of this work has been presented in [27]. In this paper, experimental results are presented. Also, disturbance estimation is considered to augment HOSM control. The approach to combat any kind of disturbance is to use a large gain for the designed control. This leads to conservative control and also amplifies the inherent disadvantage of chattering due to discontinuity in control. Use of disturbance estimation results in reducing amplitudes of discontinuous component of control, leading to the less conservative control. With this motivation, the designed STA controller is complemented with a simple DO.

To the best of our knowledge, this has been done for the first time for EHSS. The main contributions of the paper are as below:

- Detailed modeling of EHSS.
- Output feedback STA controller using relative degree one surface.
- Detailed stability proof.
- Control implementation using disturbance estimation in simulation and experimentation both.

1.2 Structure of paper

The rest of the paper is organized as follows. The mathematical modeling of the Electro-Hydraulic Servo System is elaborated in Sect. 2. Section 3 describes model validation. The control development and disturbance estimation is presented in Sect. 4. Detailed stability proof is presented in Sect. 5. The simulation results are shown in Sect. 6. Experimental set up is described in Sect. 7. Experimental results are presented in Sect. 8. Section 9 concludes the work.

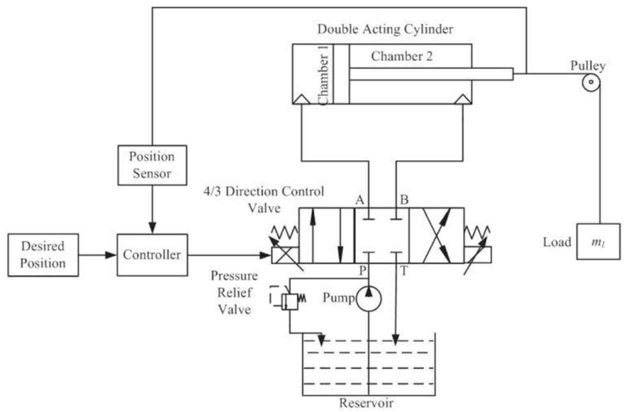

Fig. 1 Schematic of a typical EHSS

2 Mathematical modeling of electro-hydraulic servo system

A typical EHSS comprises of hydraulic fluid tank, hydraulic pump, pressure relief valve, hydraulic valve, hydraulic double actuating cylinder with single rod, load connected to hydraulic cylinder and controller. Schematic of EHSS is shown in Fig. 1.

When solenoid coil of the hydraulic valve is energized, current sets up in the coil establishes a flux. The magnetic field sets up around the coil results in an electromagnetic force (F_{mag}) on the spool of the valve. This F_{mag} causes spool displacement which in turn opens orifice. This results in pressurized fluid flow from the reservoir to the pressure ports through the proportional valve. Fluid flow in hydraulic cylinder builds up pressure on the piston. That pressure head drives the piston and subsequently the load attached to it. The load displacement is controlled by controlling voltage applied to the solenoid coil.

In [27], the mathematical model developed by Shailaja et al. [28,29] has been modified to reduce the complexity and to solve singularity issue. The model reported in [27] has been revisited here. Total EHSS dynamics include Solenoid Valve Dynamics, Spool Dynamics, Pressure Dynamics and Load Dynamics.

2.1 Assumptions in modeling

Following assumptions are considered while developing the model.

- Return line pressure is neglected.
- Orifices are matched and symmetrical.
- Fluid flow is incompressible and laminar.
- Frictional force between the cylinder wall and the piston is neglected. This is due to the fact that frictional forces acting on piston are very small in magnitude as compared to load forces on cylinder.
- Leakage flow of fluid in the cylinder and the valve is neglected. Decrease in the flow rate due to these leakages are very less hence those leakages can be overlooked.

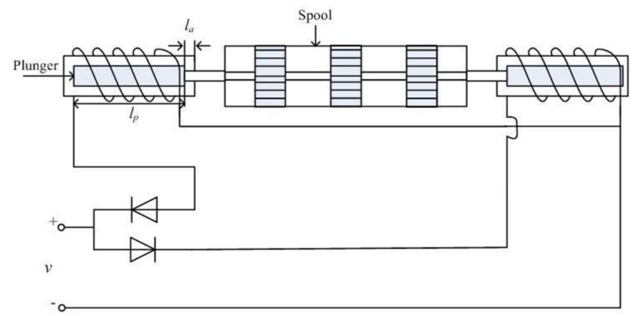

Fig. 2 Flux established in the solenoid coil

2.2 Solenoid valve dynamics

The electro-hydraulic valve comprises of the solenoid coil and spool-plunger arrangement as shown in Fig. 2. The energized solenoid coil creates a F_{mag} on the plunger. When plunger moves, reluctance offered to flux varies and hence inductance varies as a function of spool displacement [2].

Looking at the geometry as shown in Fig. 2, length of air gap hence reluctance offered by it changes as spool gets displaced. Thus the total reluctance offered by an air gap and the ferromagnetic plunger is,

$$R_l = \frac{l_a - x_s}{\mu_0 A_p} + \frac{l_p}{\mu_0 \mu_r A_p} = \frac{-x_s}{\mu_0 A_p} + \frac{l_a \mu_r + l_p}{\mu_0 \mu_r A_p}, \tag{1}$$

which can be written as,

$$R_l = R_2 - R_1 x_s. \tag{2}$$

where $R_1 = \frac{1}{\mu_0 A_p}$ and $R_2 = \frac{l_a \mu_r + l_p}{\mu_0 \mu_r A_p}$.

Since R_l is the function of x_s, inductance is also function of x_s and is given by [2],

$$L_{x_s} = \frac{N^2}{R_l} = \frac{N^2}{R_2 - R_1 x_s}. \tag{3}$$

Therefore,

$$\frac{dL_{x_s}}{dx_s} = \frac{R_1 N^2}{(R_2 - R_1 x_s)^2}. \tag{4}$$

Kirchhoff's Voltage Law is applied to coil having above inductance and resistance R, with v as applied voltage,

$$v = iR + L_{x_s}\frac{di}{dt} + i\frac{dL_{x_s}}{dx_s}\frac{dx_s}{dt}, \tag{5}$$

substituting L_{x_s} and $\frac{dL_{x_s}}{dx_s}$ from Eqs. (3) and (4) in above equation,

$$v = iR + \frac{N^2}{(R_2 - R_1 x_s)}\frac{di}{dt} + i\frac{R_1 N^2}{(R_2 - R_1 x_s)^2}\frac{dx_s}{dt}. \tag{6}$$

Rearranging above equation to get,

$$\frac{di}{dt} = \frac{(R_2 - R_1 x_s)}{N^2}\left[v - iR - i\frac{R_1 N^2}{(R_2 - R_1 x_s)^2}\frac{dx_s}{dt}\right]. \tag{7}$$

Using Eq. (2), the dynamic equation becomes,

$$\frac{di}{dt} = \frac{R_l}{N^2}\left[v - iR - i\frac{R_1 N^2}{{R_l}^2}\frac{dx_s}{dt}\right]. \tag{8}$$

2.3 Spool dynamics

Excited coil produces F_{mag} on the spool-plunger assembly. This force is given by,

$$F_{mag} = \frac{i^2 N^2 R_1}{2(R_2 - R_1 x_s)^2}. \tag{9}$$

Using Eq. (2), the above equation becomes,

$$F_{mag} = \frac{i^2 N^2 R_1}{2{R_l}^2}. \tag{10}$$

This F_{mag} displaces the spool to initiate orifice opening. This motion is opposed by flow forces. The spool motion is given by,

$$F_{mag} = m_s\frac{d^2 x_s}{dt^2} + b\frac{dx_s}{dt} + kx_s + F_{flow}, \tag{11}$$

where F_{flow} are flow forces which are negligible and hence neglected in dynamics.

From Eqs. (10) and (11) spool dynamics is,

$$\frac{d^2 x_s}{dt^2} = \frac{i^2 N^2 R_1}{2(R_l)^2 m_s} - \frac{b}{m_s}\frac{dx_s}{dt} - \frac{k}{m_s}x_s. \tag{12}$$

2.4 Pressure dynamics

When orifice opening is initiated, pressurized fluid flows from reservoir to hydraulic cylinder as shown in Fig. 3. This results in variation of volume in the hydraulic cylinder which further results in change in pressure.

Due to pressurized fluid flow through pressure port A, differential pressure is established in the cylinder. This exerts a force on the piston. During this process volume, flow rate and pressure in chamber 1 and 2 of the hydraulic cylinder varies.

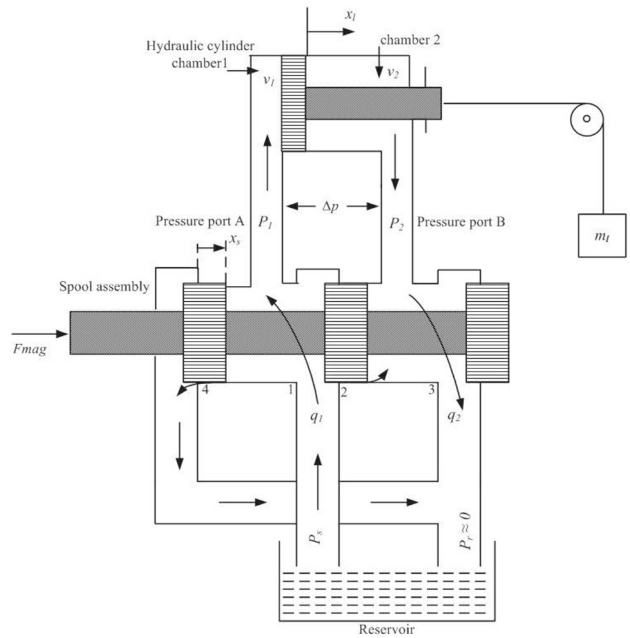

Fig. 3 Pressure and flow dynamics in EHSS

Flow rates in the cylinder that vary due to variations in x_s are,

$$q_1 = c_d \omega x_s \sqrt{\left(\frac{p_s - p_1}{\rho}\right)} \text{ and } q_2 = c_d \omega x_s \sqrt{\left(\frac{p_2}{\rho}\right)}.$$

The pressure dynamics in chamber 1 and 2 are,

$$\dot{p}_1 = \frac{\beta}{v_1 + v_{p1}}\left(q_1 - A_a\frac{dx_l}{dt}\right), \tag{13}$$

$$\dot{p}_2 = \frac{\beta}{v_2 + v_{p2}}\left(-q_2 + A_b\frac{dx_l}{dt}\right), \tag{14}$$

where $v_1 = v_i + A_a x_l$ and $v_2 = v_f - A_b x_l$.

Since the cylinder used is asymmetrical double acting cylinder, the differential pressure is,

$$\Delta p = p_1 - np_2. \tag{15}$$

where $n = \frac{A_b}{A_a}$

$$\frac{d\Delta p}{dt} = \dot{p}_1 - n\dot{p}_2. \tag{16}$$

Substituting for $\dot{p}_1$ and $\dot{p}_2$ from Eqs. (13) and (14),

$$\frac{d\Delta p}{dt} = \frac{\beta c_d \omega x_s}{\sqrt{\rho}}\left[\frac{\sqrt{p_s - p_1}}{v_1 + v_{p1}} - \frac{n\sqrt{p_2}}{v_2 + v_{p2}}\right] - \beta\frac{dx_l}{dt}\left[\frac{A_a}{v_1 + v_{p1}} - \frac{nA_b}{v_2 + v_{p2}}\right]. \tag{17}$$

2.5 Load dynamics

The force exerting on load m_l is,

$$F_g = A_a p_1 - A_b p_2. \tag{18}$$

This force causes the load motion, the governing dynamic equation is,

$$F_g = m_l \frac{d^2 x_l}{dt^2} + b_l \frac{dx_l}{dt}, \tag{19}$$

where b_l is coefficient of friction.

From Eqs. (18) and (19) load dynamics is given by,

$$\frac{d^2 x_l}{dt^2} = \frac{A_a(p_1 - np_2)}{m_l} - \frac{b_l}{m_l}\frac{dx_l}{dt} \tag{20}$$

This can be written as,

$$\frac{d^2 x_l}{dt^2} = \frac{A_a}{m_l}\Delta p - \frac{b_l}{m_l}\frac{dx_l}{dt}. \tag{21}$$

It may be noted that, if applied voltage becomes zero, due to spring action, x_s becomes zero. As soon as $x_s = 0$, ports A, B, P and T in spool plunger assembly shown in Fig. 1 are remain intact. Hence ΔP remain constant even if control voltage is removed. Therefore, load will not sink and its position will be maintained.

Defining $i = x_1$, $x_s = x_2$, $\dot{x}_s = x_3$, $\Delta p = x_4$, $x_l = x_5$, $\dot{x}_l = x_6$, and $v = u$. From Eqs. (8), (12), (17) and (21) the complete plant dynamics in state space can be represented as,

$$\dot{x}_1 = \frac{R_l}{N^2}\left[u - x_1 R - x_1 \frac{R_1 N^2}{{R_l}^2} x_3\right] \tag{22a}$$

$$\dot{x}_2 = x_3 \tag{22b}$$

$$\dot{x}_3 = \frac{x_1^2 N^2 R_1}{2{R_l}^2 m_s} - \frac{b}{m_s}x_3 - \frac{k}{m_s}x_2 \tag{22c}$$

$$\dot{x}_4 = \frac{\beta c_d \omega x_2}{\sqrt{\rho}}\left[\frac{\sqrt{p_s - p_1}}{v_1 + v_{p_1}} - \frac{n\sqrt{p_2}}{v_2 + v_{p_2}}\right] - \beta x_6 \left[\frac{A_a}{v_1 + v_{p_1}} - \frac{nA_b}{v_2 + v_{p_2}}\right] \tag{22d}$$

$$\dot{x}_5 = x_6 \tag{22e}$$

$$\dot{x}_6 = \frac{A_a}{m_l}x_4 - \frac{b_l}{m_l}x_6 \tag{22f}$$

Remark I This model is generalized model for 1 DoF EHSS. It does not consider state and control constraints. The physical parameters and constants of the system are given in Table 1.

Table 1 Physical parameters and constants of system

Parameters	Values	Units
R_1	7037	mho
R_2	7142	mho
$x_{s\,max}$	2.5×10^{-3}	m
R	3.2	Ω
N	1000	–
b	100	Ns/m
k	1200	N/m
m_s	0.5	kg
b_l	400	Ns/m
m_l	10	kg
β	1.64×10^6	Pa
ρ	880	kg/m^3
C_d	0.6	–
ω	0.024	m^2/m
p_s	3×10^6	Pa
A_a	0.001256	m^2
A_b	0.001002	m^2
v_i	6.283×10^{-6}	m^3
v_f	37.69×10^{-4}	m^3
v_{p_1}	3.958×10^{-4}	m^3
v_{p_2}	3.298×10^{-4}	m^3
A_p	113.09×10^{-6}	m^2
l_p	30×10^{-3}	m
l_a	1×10^{-3}	m
μ_0	$4\Pi \times 10^{-7}$	H/m
μ_r	2000	H/m

3 Model validation

The mathematical model developed in Eq. (22) has been validated. The proposed model was simulated in Matlab. The system model was excited by the step input of amplitude 5 V. The actual plant was also excited by same input of 5 V. Figure 4 shows the response of the model and actual system for the step input. To validate the model simulated performance is compared with the experimental performance by exciting the actual system using the same step command. It is observed that system excitation delay of the order of 0.7751 s. is negligible compared to system time constant i.e. 5.985 s. and desired settling time. Hence it is neglected while designing the controller. Further pulse input of amplitude 5 V and time period 10 and pulse width 20% of the time period was considered as an input. Figure 5 shows the response of the model and actual plant to pulse input. It can be seen that the proposed model fairly captures system dynamics.

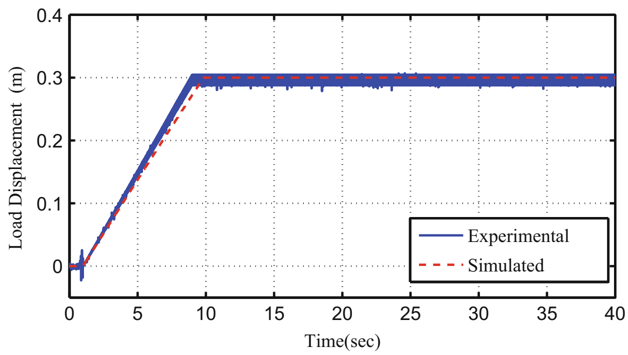

Fig. 4 Response of system to step input

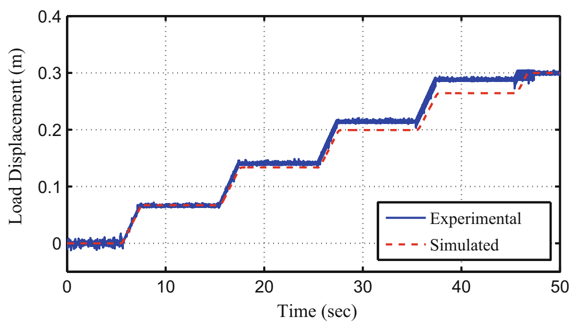

Fig. 5 Response of system to pulse input

Remark II Model in Eq. (22) is detailed and general. Consideration of constraints due to geometry and design constraints, this model can be simplified as explained subsequently.

It may be noted that due to geometry of valve when plunger movement is initiated the spool can move a maximum distance of ± 2.5 mm. Hence spool position $x_2 \in [-2.5 \times 10^{-3}, + 2.5 \times 10^{-3}]$. Therefore R_l which is $(R_2 - R_1 x_s)$ lies in [7124.41, 7159.59]. Using this information and system parameters and constants given in Table 1 we get,

$$\frac{R_l}{N^2} \equiv a_1 \in [7.124, 7.159] \times 10^{-3},$$
$$R\left[\frac{R_l}{N^2}\right] \equiv a_2 \in [22.79, 22.91] \times 10^{-3},$$
$$\frac{R_1}{R_l} \equiv a_3 \in [0.9828, 0.9876],$$
$$\frac{N^2 R_1}{2{R_l}^2 m_s} \equiv a_4 \in [137.268, 138.628],$$
$$\frac{b}{m_s} \equiv a_5 = 200,$$
$$\frac{k}{m_s} \equiv a_6 = 2400.$$

Similarly pressures p_1 and p_2 can vary from 0 to p_s due to variation in x_s. Therefore

$$\frac{\beta c_d \omega}{\sqrt{\rho}}\left[\frac{\sqrt{p_s - p_1}}{v_1 + v_{p_1}} - \frac{n\sqrt{p_2}}{v_2 + v_{p_2}}\right] \equiv a_7 \in [315.55, 0] \times 10^7,$$
$$\beta\left[\frac{A_a}{v_1 + v_{p_1}} - \frac{nA_b}{v_2 + v_{p_2}}\right] \equiv a_8 \in 1.64 \times 10^6 [2.9, 1.4].$$

Other constants are

$$\frac{A_a}{m_l} \equiv a_9 = 0.0001256,$$
$$\frac{b_l}{m_l} \equiv a_{10} = 40.$$

Therefore Eq. (22) is represented as interval system with a_1 to a_4, a_7 and a_8 being parameters lying in certain interval. Further a_5, a_6, a_9 and a_{10} are constants. The dynamics is

$$\dot{x}_1 = a_1 u - a_2 x_1 - a_3 x_1 x_3 \tag{23a}$$
$$\dot{x}_2 = x_3 \tag{23b}$$
$$\dot{x}_3 = a_4 {x_1}^2 - a_5 x_3 - a_6 x_2 \tag{23c}$$
$$\dot{x}_4 = a_7 x_2 - a_8 x_6 \tag{23d}$$
$$\dot{x}_5 = x_6 \tag{23e}$$
$$\dot{x}_6 = a_9 x_4 - a_{10} x_6 \tag{23f}$$

The sixth order model in Eq. (23) is nonlinear and uncertain.

Remark III Control design for this uncertain system is hard. Control becomes complex and unimplementable if such model is considered for control design. Moreover all the states are not measurable. This creates problem in implementing modern control which needs information of all the states.

The model in Eq. (23) is further simplified as described below:

Substituting x_6 from Eq. (23d) in Eq. (23f),

$$\dot{x}_6 = a_9 x_4 - a_{10}\left[\left(\frac{a_7}{a_8}\right)x_2 - \left(\frac{1}{a_8}\right)\dot{x}_4\right]. \tag{24}$$

From Eq. (23c), x_2 is represented as,

$$x_2 = -\frac{1}{a_6}\left(-a_4 {x_1}^2 + a_5 x_3 + \dot{x}_3\right).$$

Now substituting x_2 in Eq. (24),

$$\dot{x}_6 = a_9 x_4 + \left(\frac{a_{10} a_7}{a_8 a_6}\right)\left(-a_4 {x_1}^2 + a_5 x_3 + \dot{x}_3\right) + \left(\frac{a_{10}}{a_8}\right)\dot{x}_4. \tag{25}$$

Multiplying Eq. (23a) by x_1, and rearranging to get,

$$x_1{}^2 = -\left(\frac{1}{a_2}\right) x_1\dot{x}_1 - \left(\frac{a_3}{a_2}\right) x_1{}^2 x_3 + \left(\frac{a_1}{a_2}\right) u x_1.$$

Defining $\frac{a_{10}a_7}{a_8a_6} = a_{12}$, $\frac{a_{10}}{a_8} = a_{13}$ and substituting x_1^2 in Eq. (25) we get,

$$\dot{x}_6 = a_9x_4 + a_{12}\left[-a_4\left(-\frac{1}{a_2}x_1\dot{x}_1 - \frac{a_3}{a_2}x_1{}^2x_3 + \frac{a_1}{a_2}ux_1\right)\right] + a_{12}a_5x_3 + a_{12}\dot{x}_3 + a_{13}\dot{x}_4. \tag{26}$$

Substituting $\dot{x}_3$ from Eq. (23c) and $\dot{x}_4$ from Eq. (23d) in Eq. (26) to get,

$$\begin{aligned}\dot{x}_6 = a_9x_4 - a_{12}a_4\left(-\frac{1}{a_2}x_1\dot{x}_1 - \frac{a_3}{a_2}x_1{}^2x_3 + \frac{a_1}{a_2}ux_1\right)\\ + a_{12}a_5x_3 + a_{12}(a_4x_1{}^2 - a_5x_3 - a_6x_2)\\ + a_{13}(a_7x_2 - a_8x_6).\end{aligned} \tag{27}$$

Rearranging the above equation to get,

$$\begin{aligned}\dot{x}_6 = a_{12}a_4x_1{}^2 - (a_{12}a_6 - a_{13}a_7)x_2 - a_{13}a_8x_6\\ + \left(\frac{a_{12}a_4}{a_2}\right)x_1\dot{x}_1 + \left(\frac{a_{12}a_4a_3}{a_2}\right)x_1{}^2x_3 + a_9x_4\\ - \left(\frac{a_{12}a_4a_1}{a_2}\right)ux_1.\end{aligned} \tag{28}$$

Now defining $\frac{a_{12}a_4}{a_2} = a_{14}$ the above can be written as,

$$\begin{aligned}\dot{x}_6 = a_{12}a_4x_1{}^2 - (a_{12}a_6 - a_{13}a_7)x_2 - a_{13}a_8x_6\\ + a_{14}x_1\dot{x}_1 + a_{14}a_3x_1{}^2x_3 + a_9x_4 - a_{14}a_1x_1u.\end{aligned} \tag{29}$$

Equation (29) can be rearranged as below:

$$\begin{aligned}x_6 = \frac{1}{a_{13}a_8}(a_{12}a_4x_1{}^2 - (a_{12}a_6 - a_{13}a_7)x_2 - \dot{x}_6\\ + a_{14}x_1\dot{x}_1 + a_{14}a_3x_1{}^2x_3 + a_9x_4 - a_{14}a_1x_1u).\end{aligned} \tag{30}$$

Now substituting $\frac{1}{a_{13}a_8} = a_{15}$ and using Eq. (23e), above becomes,

$$\begin{aligned}\dot{x}_5 = a_{15}a_{12}a_4x_1{}^2 - a_{15}(a_{12}a_6 - a_{13}a_7)x_2 - a_{15}\dot{x}_6\\ + a_{15}a_{14}x_1\dot{x}_1 + a_{15}a_{14}a_3x_1{}^2x_3 + a_{15}a_9x_4\\ - a_{15}a_{14}a_1x_1u.\end{aligned} \tag{31}$$

It may be noted that supply pressure is constant (3×10^6 Pa). Volume of cylinder is also bounded. Therefore differential pressure hence force acting on load is bounded. The term a_{15} is also bounded.

Therefore $a_{15}\dot{x}_6$ defined as ψ, where ψ is bounded.

Defining,

$$\begin{aligned}a_{15}a_{12}a_4x_1{}^2 - a_{15}(a_{12}a_6 - a_{13}a_7)x_2 + a_{15}a_{14}x_1\dot{x}_1\\ + a_{15}a_{14}a_3x_1{}^2x_3 + a_{15}a_9x_4 = f(x_1, \dot{x}_1, x_2, x_3, x_4).\end{aligned}$$

The above equation can be written as,

$$\dot{x}_5 = f(x_1, \dot{x}_1, x_2, x_3, x_4) - \psi - a_{15}a_{14}a_1x_1u,$$

Since a_{14}, a_{15}, a_1, x_1 are bounded. Hence $(-a_{15}a_{14}a_1x_1u)$ can be written as $u + \Delta u$.

Therefore,

$$\begin{aligned}\dot{x}_5 = f(x_1, \dot{x}_1, x_2, x_3, x_4) - \psi + u + \Delta u,\\ \dot{x}_5 = u + \rho.\end{aligned} \tag{32}$$

where $\rho = f(x_1, \dot{x}_1, x_2, x_3, x_4) - \psi + \Delta u$.

It may be noted that ρ takes account of parametric uncertainties which includes effect of variation of temperature, pressure, etc. In presence of external matched disturbance, above equation takes the form

$$\dot{x}_5 = u + \rho + d, \tag{33}$$

where d is used to represent neglected dynamics such as time delay. Also, d is assumed to be smooth and bounded.

Remark IV EHSS exhibits time delay of the order of 0.7751 s. which is very much less than desired settling time which is order of 15–17 s.

The system in Eq. (33) is relative degree one system and is considered for control design under the valid assumption of bounded acceleration. Therefore Super Twisting Algorithm (STA) can be applied.

It may be noted that state x_1 i.e. input current is bounded hence resulting $Fmag$ acting on the spool is bounded. Similarly spool displacement x_s i.e. state x_2 and spool velocity $\dot{x}_s$ i.e. x_3 are bounded due to the geometry of spool plunger assembly and bounded magnetizing force respectively. Moreover, due to finite port opening p_1, p_2 and hence $\Delta p = x_4$ is bounded. Due to the geometry of cylinder and piston force acting on the piston is bounded hence load velocity (x_6) is bounded. Maximum load displacement (x_5) is equal to piston length which is finite hence the load displacement is bounded. Thus it is evident that all states are bounded.

4 Control development

The control objective is to design second order sliding mode controller for complex EHSS described in Eq. (22) to move 10 kg mass through 0.1 m in 17 s. The state x_5 i.e. actual load position is measurable whereas other states x_1, x_2, x_3, x_4 and x_6 are not measurable. A simple linear sliding variable is proposed.

$$\sigma_l = e_{x_5}, \tag{34}$$

where $e_{x_5} = x_5 - x_{5_d}$.

Here, x_{5_d} is desired load position. Differentiating Eq. (34),

$$\dot{\sigma}_l = \dot{e}_{x_5}, \tag{35}$$

Now surface in Eq. (34) is relative degree one surface with respect to Eq. (32). Therefore Super Twisting Algorithm (STA) can be applied.

According to STA [24], the variable σ_1 and its derivative $\dot{\sigma}_l$ converge to zero in finite time if $\dot{\sigma}_l = -k_1|\sigma_l|^{0.5} sgn(\sigma_l) - k_2 \int sgn(\sigma_l) + \rho_l$ with $k_2 > |\rho_l|_{max}$, $k_1 > k_2$.

Differentiating Eq. (34) to get

$$\dot{\sigma}_l = \dot{x}_5 = x_6. \tag{36}$$

Therefore using Eq. (32)

$$\dot{\sigma}_l = u + \rho + d. \tag{37}$$

With the choice of u as

$$u = -k_1|\sigma_l|^{0.5} sgn(\sigma_l) - k_2 \int_0^t sgn(\sigma_l) d\tau, \tag{38}$$

σ_l and $\dot{\sigma}_l$ converges to zero in finite time if $k_2 > (|\rho|_{max} + |d|_{max})$ and $k_1 > k_2$. $|\rho|_{max}$ can be calculated using worst case analysis and $|d|_{max}$ is assumed to be known [24]. Other methods such as evolutionary algorithm can also be found to arrive at controller gains k_1 and k_2.

4.1 Disturbance estimation

The STA based control designed in Eq. (38) is developed to compensate for the disturbance via appropriately assumed gains. These high gains can be avoided if an approximate estimate of the disturbance is available. In this section Disturbance Observer (DO) is designed to estimate the unknown lumped disturbance. The Eq. (33) can be represented as,

$$\dot{x}_5 = u + x_5 + \rho + d - x_5$$

Defining $\rho + d - x_5 = \rho_d$,

$$\dot{x}_5 = u + x_5 + \rho_d$$

The estimate of ρ_d is obtained with simple inversion of dynamics i.e.;

$$\hat{\rho}_d = \dot{x}_5 - x_5 - u \tag{39}$$

Here $\hat{\rho}_d$ is the estimate of the disturbance. x_5 is measurable and u is the known input. However, $\dot{x}_5$ is unknown. It is proposed to obtain information of $\dot{x}_5$ using a HOSM exact differentiator. The exact first order differentiator as proposed by Levant in [30] is used as follows;

$$\begin{aligned} \dot{\hat{x}}_5 &= \nu + w_1 \\ \dot{\nu} &= w_2, \end{aligned} \tag{40}$$

The correction variables w_1 and w_2 are output injections of the form;

$$\begin{aligned} w_1 &= \lambda |x_5 - \hat{x}_5|^{1/2} sign(x_5 - \hat{x}_5) \\ w_2 &= \alpha sign(x_5 - \hat{x}_5) \end{aligned}$$

λ and α are the tuning parameters. The DO is thus modified to have the form

$$\hat{\rho}_d = \dot{\hat{x}}_5 - x_5 - u \tag{41}$$

The HOSM differentiator provides exact, finite time convergent derivative of x_5. It thus removes the necessity of filter and its allied disadvantages as in a conventional DO.

$\hat{\rho}_d$ is estimate of $\rho + d - x_5$.

Therefore, estimate of $(\rho + d)$ i.e. $\hat{\rho} + \hat{d} = \hat{\rho}_d + x_5$.

4.2 Proposed controller with disturbance estimation

The proposed controller in Eq. (38) is augmented to compensate the disturbance. The control law therefore becomes

$$u_1 = -k_1|\sigma_l|^{0.5} sgn(\sigma_l) - k_2 \int_0^t sgn(\sigma_l) d\tau - (x_5 + \hat{\rho}_d), \tag{42}$$

This is proposed controller with proposed disturbance estimator. This controller is compared with the STA controller using non-singular terminal sliding surface [31], which is also finite time controller.

4.3 Controller with non-singular terminal sliding surface

Non-singular terminal sliding surface is

$$\sigma_2 = e_{x_5} + \beta_1 \dot{e}_{x_5}^{\frac{5}{3}}, \tag{43}$$

where $\dot{e}_{x_5} = \dot{x}_5 - \dot{x}_{5_d} = \dot{x}_5$.

Here $\dot{x}_5$ and $\dot{x}_{5_d}$ are actual and desired load velocity respectively. Now STA controller using surface σ_2 is

$$u_2 = -k_3|\sigma_2|^{0.5} sgn(\sigma_2) - k_4 \int_0^t sgn(\sigma_2) d\tau, \tag{44}$$

where k_3 and k_4 are controller gains so chosen to ensure sliding. Proposed output feedback finite time controller in Eq. (42) is compared with finite time controller in Eq. (44). Finite time convergence is explained in next subsection for the sake of ready reference.

4.4 Existence of sliding

Theorem 1 *Control in Eq. (38) ensures $\sigma_l = \dot{\sigma}_l = 0$ in finite time if $k_1 > k_2 > |\rho|_{max} + |d|_{max}$.*

Proof Define $\sigma_l = z_1$.

Differentiating the above

$$\dot{\sigma}_l = \dot{z}_1.$$

Using Eq. (37) and substituting u from Eq. (38), the above equation becomes $\dot{z}_1 = -k_1|z_1|^{0.5}sgn(z_1) - k_2\int sgn(z_1) + \rho_l$.

Defining $\rho + d = \rho_l$,

$$\dot{z}_1 = -k_1|z_1|^{0.5}sgn(z_1) + z_2 + \rho_l$$
$$\dot{z}_2 = -k_2 sgn(z_1)$$

This is classical STA in z_1. Therefore z_1 and $\dot{z}_1$ (i.e. σ_l and $\dot{\sigma}_l$) converge to zero in finite time [32] if $k_1 > k_2 > |\rho_l|_{max}$.

Similarly, it can be proved that controller in Eq. (44) ensures sliding if $k_3 > k_4 > |\rho_l|_{max}$. □

5 Stability analysis

This section illustrates stability analysis of system with the proposed controller.

STA controller ensures σ_l and $\dot{\sigma}_1$ zero in finite time.

Therefore from Eqs. (34) and (35),

$$e_{x_5} = e_{x_l} = 0, \tag{45}$$
$$\dot{e}_{x_5} = \dot{e}_{x_l} = 0. \tag{46}$$

With this x_l acquires x_{ld} and $\dot{x}_l = 0$ in finite time. Since, $\dot{x}_l = 0$; forcing function exerting on load is zero i.e. $A_a\Delta p \to 0$. This implies that $\Delta p \to 0$ and $\Delta\dot{p} \to 0$. When $\Delta p \to 0$, $p_1 \cong p_2$ and change in volume of chamber 1 (v_1) and chamber 2 (v_2) tends to zero. There is no further change in orifice area hence $q_1 \cong q_2$. Constant flow means no further spool motion. This implies that forcing function acting on spool i.e. $Fmag \to 0$ which in turn implies that $i \to 0$. From Eq. (12), x_s and $\dot{x}_s$ converges to zero asymptotically. Thus $\dot{x}_l$ converges to zero in finite time and all remaining states converge asymptotically.

Another method is proposed to prove stability of the system.

Theorem 2 *Finite time convergence of the proposed sliding surface in Eq. (34) with control in Eq. (42) ensures the convergence of all the states with finite time convergence of load to desired position and its velocity to zero if $k' > 2.018$.*

Proof Choosing the Lyapunov function as below.

$$V = \frac{a_4{x_1}^2}{2a_3} + a_6\frac{{x_2}^2}{2} + \frac{{x_3}^2}{2} + \frac{{x_4}^2}{2} + k'|\sigma_l| + \frac{{x_6}^2}{2},$$

Since a_3, a_4, a_6 and k' are positive the above is valid Lyapunov function.

Differentiating the above

$$\dot{V} = \left(\frac{a_4}{a_3}\right)x_1\dot{x_1} + a_6x_2\dot{x_2} + x_3\dot{x_3} + x_4\dot{x_4} + k'(sgn\sigma_l)\dot{\sigma}_l + x_6\dot{x}_6.$$

Using Eq. (23), the above becomes,

$$\dot{V} = \left(\frac{a_4}{a_3}\right)x_1(a_1u - a_2x_1 - a_3x_1x_3) + a_6x_2x_3 + x_3(a_4{x_1}^2 - a_5x_3 - a_6x_2) + x_4(a_7x_2 - a_8x_6) + k'(sgn\sigma_l)\dot{\sigma}_l + x_6(a_9x_4 - a_{10}x_6).$$

Simplifying the above to get,

$$\dot{V} = \left(\frac{a_4a_1}{a_3}\right)x_1u - \left(\frac{a_4a_2}{a_3}\right){x_1}^2 - a_5{x_3}^2 + a_7x_2x_4 + (a_9 - a_8)x_4x_6 + k'(sgn\sigma_l)\dot{\sigma}_l - a_{10}{x_6}^2.$$

All parameters from a_1 to a_{10} are positive uncertain constants. When $x_2 > 0$, $x_4 > 0$ and $a_7 < 0$ also when $x_2 < 0$, $x_4 > 0$ and $a_7 > 0$. Therefore $a_7x_2x_4$ is either zero or negative definite. Similarly when $x_4 > 0$, $x_6 > 0$ and when $x_4 < 0$, $x_6 < 0$. Therefore $x_4x_6 > 0$. Further $a_8 >> a_9$ therefore the term $(a_9 - a_8)x_4x_6$ is always negative definite. Therefore $\dot{V} < 0$ if

$$\left(\frac{a_4a_1}{a_3}\right)x_1u + k'sgn(\sigma_l)\dot{\sigma}_l < 0.$$

Now defining $\left(\frac{a_4a_1}{a_3}\right) = a_{11}$ and substituting for u from Eq. (38) in above, $\dot{V} < 0$ if

$$a_{11}x_1(-k_1|\sigma_l|^{0.5}sgn(\sigma_l) - k_2\int_0^t sgn(\sigma_l)d\tau) + k'sgn(\sigma_l)\dot{\sigma}_l < 0.$$

It may be noted that for positive σ_l, $\dot{\sigma}_l$ is negative and for negative σ_l, $\dot{\sigma}_l$ is positive leading to $k'sgn\sigma_l\dot{\sigma}_l$ negative. Therefore $\dot{V} < 0$ if

$$|k'sgn(\sigma_l)\dot{\sigma}_l| > |a_{11}x_1u|. \tag{47}$$

Since $k' > 0$ and $|sgn\sigma_l| = 1$, the above condition becomes

$$k'|\dot{\sigma}_l| > |a_{11}x_1|_{max}|u|$$

Considering maximum rated value of current i.e. $x_{1_{max}} = 2A$ and the parameters a_1, a_3 and a_4 from Table I, $a_{11_{max}} = 1.009$. For $\dot{V} < 0$,

$$k'|\dot{\sigma}_l| > 2.018|u| \tag{48}$$

If condition in Eq. (48) is satisfied for any controller then that controller stabilizes all the states which implies that during reaching (i.e. $\sigma_l \to 0$) all other states also converge.

Controller in Eqs. (38), (42) and (44) can be analyzed for stability by verifying condition in Eq. (48) for possibility of negative definiteness of $\dot{V}$.

Substituting Eq. (38) in Eq. (48), $\dot{V} < 0$ if

$$k'|\dot{\sigma}_l| > 2.018\left|-k_1|\sigma_l|^{0.5}sgn(\sigma_l) - k_2\int_0^t sgn(\sigma_l)d\tau\right|.$$

As per STA, $\dot{\sigma}_l = -k_1|\sigma_l|^{0.5}sgn(\sigma_l) - k_2\int_0^t sgn(\sigma_l)d\tau + \rho_l$.

Therefore, $\dot{V} < 0$ if,

$$k'|\dot{\sigma}_l| > 2.018|(\dot{\sigma}_l - \rho_l)|.$$

where ρ_l is total lumped disturbance.

If $k'|\dot{\sigma}_l| > 2.018|\dot{\sigma}_l|$ then $k'|\dot{\sigma}_l| > 2.018|\dot{\sigma}_l| - 2.018|\rho_l|_{max}$.

Therefore for $\dot{V} < 0$; $k'|\dot{\sigma}_l| > 2.018|\dot{\sigma}_l|$, it implies that if $k' > 2.018$ then stability is assured. Hence with $k' > 2.018$ proposed output feedback controller without estimation ensures convergence of all states.

Similarly stability with controller in Eq. (42) is verified.

Substituting Eq. (42) in Eq. (48),

$$\dot{V} < 0, \text{if}$$
$$k'|\dot{\sigma}_l| > \eta\left|-k_1|\sigma_l|^{0.5}sgn(\sigma_l) - k_2\int_0^t sgn(\sigma_l) - (x_5 + \hat{\rho}_d)\right|$$

where $\eta = 2.018$. Now, $\hat{\rho}_d$ is estimate of $\rho + d + x_5$ hence $x_5 + \hat{\rho}_d = \hat{\rho} + \hat{d}$.

Therefore $\dot{V} < 0$ if

$$k'|\dot{\sigma}_l| > 2.018| - k_1|\sigma_l|^{0.5}sgn(\sigma_l)$$
$$- k_2\int_0^t sgn(\sigma_l)d\tau - (\hat{\rho} + \hat{d})|.$$

$(\rho + d)$ is lumped disturbance is equal to ρ_l. Therefore for $\dot{V} < 0$,

$$k'|\dot{\sigma}_l| > 2.018\Big|-k_1|\sigma_l|^{0.5}sgn(\sigma_l)$$
$$- k_2\int_0^t sgn(\sigma_l)d\tau - \rho_l\Big|.$$

According to STA,

$$-k_1|\sigma_l|^{0.5}sgn(\sigma_l) - k_2\int_0^t sgn(\sigma_l)d\tau + \rho_l = \dot{\sigma}_l.$$

Hence for $\dot{V} < 0$, $k'|\dot{\sigma}_l| > 2.018|\dot{\sigma}_l|$ which means $k' > 2.018$ ensures stability. Thus with $k' > 2.018$ proposed output feedback controller with proposed estimation ensures convergence of all states.

For devising controller in Eq. (44), sliding variable is σ_2 instead of σ_l. Accordingly derivation of Lyapunov function is negative definite if $k'|\dot{\sigma}_2| > 2.018|u_2|$.

Substituting u_2 from Eq. (44), $\dot{V} < 0$ if

$$k'|\dot{\sigma}_2| > 2.018\left|-k_3|\sigma_2|^{0.5}sgn(\sigma_2) - k_4\int_0^t sgn(\sigma_2)d\tau\right|.$$

As per STA,

$$\dot{\sigma}_2 = -k_3|\sigma_2|^{0.5}sgn(\sigma_2) - k_4\int_0^t sgn(\sigma_2)d\tau + \rho_l.$$

Therefore for $\dot{V} < 0$; $k'|\dot{\sigma}_2| > 2.018|(\dot{\sigma}_2 - \rho_l)|$.

If $k'|\dot{\sigma}_2| > 2.018|\dot{\sigma}_2|$ then $k'|\dot{\sigma}_2| > 2.018|\dot{\sigma}_2| - 2.018|\rho_l|_{max}$.

Therefore for $\dot{V} < 0$; $k'|\dot{\sigma}_2| > 2.018|\dot{\sigma}_2|$, which implies that if $k' > 2.018$ then stability is assured.

Hence with $k' > 2.018$, controller in Eq. (44) ensures convergence of all states.

Without loss of generality, k' can be chosen greater than 2.018. Thus all controllers in Eqs. (38), (42) and (44) are stabilizing controllers. □

6 Simulation results

To test performance of controllers in Eqs. (42) and (44), the system in (22) and controllers were simulated in Matlab. $k_1 = 4.7$, $k_2 = 0.01$, $k_3 = 10$, $k_4 = 0.008$ and $\beta_1 = 1$ are simulation parameters. These parameters were so tuned to yield the almost same response in terms of output error stabilization. Since STA was used, control gains had to satisfy conditions that are essential for the existence of sliding. Gains k_1, k_2 of the controller in Eq. (42) and k_3, k_4 of Eq. (44) were so tuned to ensure the existence of sliding and almost same settling time of output. Step command of 0.1 was applied as the reference input. To check disturbance rejection capability sinusoidal varying external disturbance $0.1sin(4\pi t)$ was added in the input channel. Figure 6a, b shows performance with the disturbance in input channel. It is evident that performance of both controllers is robust. Also, control is smooth. Both yields load to reach at the desired position in about 17 s.

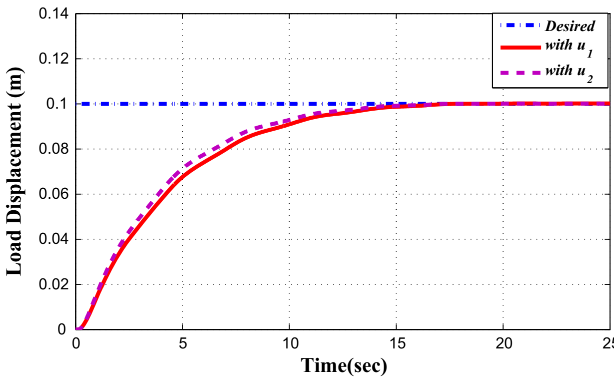

(a) Evolution of load displacement

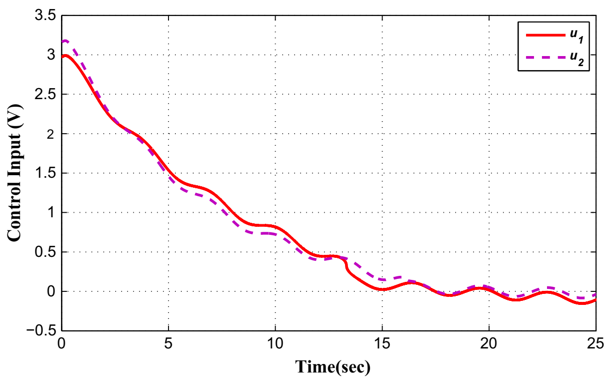

(b) Control input

Fig. 6 Controller performance in simulation. **a** Evolution of load displacement and **b** control input

7 Experimental set up

An experimental set up has been designed and developed to validate proposed method as shown in Fig. 7. It consists of hydraulic power pack, inline filter, single rod asymmetrical double acting cylinder driven by 4/3 position proportional valve Atos DHZO-AE-071-L1, oil temperature indicator, linear position transmitter, 10 kg load with pulley arrangement, dSPACE RTC 1104. Hydraulic actuators include hydraulic cylinder of dimension 40/18/300 mm and 230 V, 750 W, 1 H.P., 1425 RPM hydraulic motor.

8 Experimental results

Controllers developed in Eqs. (42) and (44) were implemented using dSPACE DS1104 real time interface. The necessary commands were given using Control Desk. Experiments were carried out on real time platform. The real-time control system was programmed using MATLAB/Simulink and gets transferred to the dSPACE board through the Real-Time Workshop. Figure 8a, b illustrate the experimental performance of controllers u_1, u_2 with external disturbance.

Fig. 7 Experimental set up of electro-hydraulic servo system

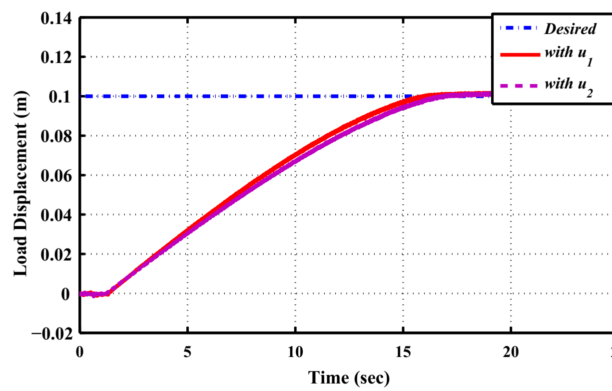

(a) Evolution of load displacement in experiment

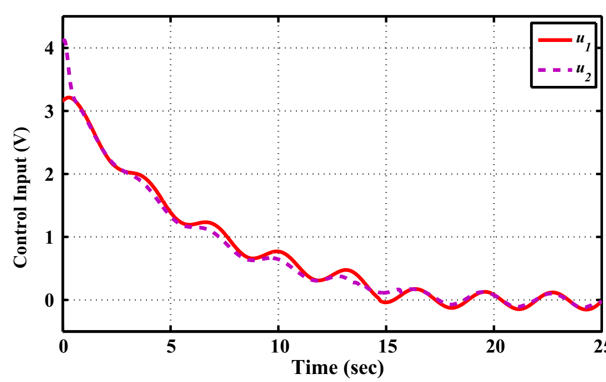

(b) Control input

Fig. 8 Controller performance in experimentation. **a** Evolution of load displacement in experiment and **b** control input

The controller gains $k_1 = 2.5$, $k_2 = 0.04$, $k_3 = 4.7$ and $k_4 = 0.056$ were chosen in experiment to get same performance in terms of settling time i.e. 17 s. The following Tables 2 and 3 illustrate quantitative comparison.

It is evident that the proposed controller with disturbance estimation shows better control quality at the cost of less control efforts. The proposed finite time output feedback controller is superior to finite time controller using non-singular terminal sliding surface.

Table 2 Quantitative comparison of proposed controller without and with estimation

	$\|\|u\|\|_2$	$\|u\|\|_\infty$	$\|\|e_(x_l)\|\|_1$
Proposed controller u_1 without estimation	359.67	2.680	791.03
Proposed controller u_1 with estimation	333.23	2.90	635.29

Table 3 Quantitative comparison of two controllers with external disturbance

	$\|\|u\|\|_2$	$\|\|u\|\|_\infty$	$\|\|e_(x_l)\|\|_1$
Proposed controller u_1 with estimation	351.37	3.21	822.88
Controller u_2 using non-singular terminal sliding surface	365.91	4.12	868.43

9 Conclusions

Relative degree one sliding surface has been proposed for devising STA controller for finite time positioning of the complex electro hydraulic servo system. Disturbance estimation and compensation has been used. Following are concluding remarks:

1. The proposed controller with disturbance compensation ensures desired robust performance.
2. The controller yields finite positioning of the load to the desired position in 17 s.
3. The proposed controller is output feedback controller. It requires information of load position. On the other hand the controller using non-singular terminal sliding surface needs information of load position and velocity.
4. The proposed controller with disturbance estimation needs control efforts 8% less than the one without estimation
5. More accuracy is observed with proposed controller.
6. Thus proposed control approach outperforms the other in terms of control quality and control energy.

References

1. Merritt HE (1967) Hydraulic control systems. Willey, New York
2. Fitzgerald AE, Kingsley C, Umans SD (2003) Electrical machinery. Mcgraw-Hill, New York
3. Kaddissi C, Kenne J-P, Saad M (2007) Identification and real-time control of an electrohydraulic servo system based on nonlinear backstepping. IEEE/ASME Trans Mechatron 12(1):12–22
4. Ling TG, Rahmat MF, Husain AR (2012) System identification and control of an electro-hydraulic actuator system. In: 2012 IEEE 8th international colloquium on signal processing and its applications, pp 85–88
5. Rahmat MF (2009) Application of self-tuning fuzzy PID controller on industrial hydraulic actuator using system identification approach. Int J Smart Sens Intell Syst 2(2):246–261
6. Pang X, Yuan Z, Zong X, Yong Q, Li J (2010) Research on neural networks based modelling and control of electrohydraulic system. Adv Comput Control 1:34–38
7. Wonohadidjojo DM, Kothapalli G, Hassan MY (2013) Position control of electro-hydraulic actuator system using fuzzy logic controller optimized by particle swarm optimization. Int J Autom Comput 10(3):181–193
8. Tripathi A, Sun Z (2016) Nonlinear feed forward control for electro hydraulic actuators with asymmetric piston areas. In: ASME 2016 dynamic systems and control conference, vol 2, October 12–14
9. Weng F, Ding Y, Tang M (2011) LPV based model-robust controller design of electro-hydraulic servo systems. Adv Control Eng Inf Sci 15:421–425
10. Niksefat N, Sepehri N (2000) Design and experimental evaluation of a robust force controller for an electro-hydraulic actuator via quantitative feedback. Control Eng Pract 8(12):1335–1345
11. Milic V, Situm Z, Essert M (2010) Robust H∞ position control synthesis of an electro-hydraulic servo system. ISA Trans 49:535–542
12. Mintsa HA, Venugopal R, Kenne J-P, Belleau C (2012) Feedback linearization-based position control of an electrohydraulic servo system with supply pressure uncertainty. IEEE Trans Control Syst Technol 20(4):1092–1099
13. Ba DX, Ahn KK, Truong DQ, Park HG (2016) Integrated model-based backstepping control for an electro-hydraulic system. Int J Precis Eng Manuf 17(5):565–577
14. Wang H, Zhang J, Li D, Wang H, Gong R (2015) Investigation on synchronous control of electro-hydraulic servo system based on MRAC. In: International conference on fluid power and mechatronics (FPM), pp 510–513
15. Edward C, Spurgeon S (1998) Sliding mode control: theory and applications. Taylor and Francis, Abingdon
16. Has Z, Rahmat M, Husain A, Ghazali R (2013) Sliding mode control with switching-gain adaptation based-disturbance observer applied to an electro-hydraulic actuator system. In: Proceedings of IEEE conference on industrial electronics and applications, pp 668–673
17. Gdoura EK, Feki M, Derbel N (2015) Sliding mode control of a hydraulic servo system position using adaptive sliding surface and adaptive gain. Int J Modell Identif Control 23(3):248–259
18. Wang S, Burton R, Habibi S (2011) Sliding mode controller and filter applied to an electrohydraulic actuator system. J Dyn Syst Meas Control 133:024504
19. Kurode S, Desai PD, Shiralkar A (2013) Modeling of electro-hydraulic servo valve and Robust Position Control using Sliding Mode Control Technique. In: Proceedings of 1st international and 16th national conference on machines and mechanisms, pp 607–614
20. Levant A (2010) Chattering analysis. IEEE Trans Autom Control 55(6):1380–1389
21. Fridman L, Moreno J, Iriarte R (2011) Sliding modes after the first decade of the 21st century, Lecture notes in control and information sciences, Chapter 4, vol 412. Springer, Berlin, pp 113–149
22. Johnson CD (1971) Accommodation of external disturbances in linear regulator and servomechanism problems. IEEE Trans Autom Control 16(6):635–644
23. Ohishi K, Nakao M, Ohnishi K, Miyachi K (1987) Microprocessor-controlled DC motor for load-insensitive position servo system. IEEE Trans Ind Electron 34(9/10):44–49
24. Levant A (1993) Sliding order and sliding accuracy in sliding mode control. Int J Control 58(6):1247–1263
25. Schmidt L, Anderson TO, Pedersen HC (2014) On application of second order sliding mode control to electro-hydraulic systems. In: ASME 2014, 12th Biennial conference on engineering systems design and analysis, vol 3

26. Azquez CV, Aranovskiy S, Freidovich L, Fridman L (2014) Second order sliding mode control of a mobile hydraulic crane. In: 53rd IEEE conference on decision and control, pp 5530–5535
27. Gore R, Shiralkar A, Kurode S (2016) Incomplete state feedback control of electro-hydraulic servo system using second order sliding modes. In: 14th International workshop on variable structure system 2016 (VSS 2016), pp 210–215
28. Shiralkar A, Kurode S (2015) Robust control of electro-hydraulic system using higher order sliding modes. In: 1st Indian control conference, pp 444–448
29. Shiralkar A, Kurode S (2016) Generalized super twisting algorithm to control electro-hydraulic servo system. IFAC-PapersOnLine 49(1):742–747
30. Levant A (2003) Higher-order sliding modes, differentiation and output-feedback control. Int J Control 76(9/10):924–941
31. Feng Y, Xinghuo Y, Man Z (2002) Non-singular terminal sliding mode control of rigid manipulators. Automatica 38:2159–2167
32. Moreno JA (2009) A linear framework for the robust stability analysis of a generalized supertwisting algorithm. In: 6th International conference on electrical engineering, computer science and automatic control (CCE 2009), pp 12–17, Mexico